Research Journal of Engineering Sciences ISSN 2278 – 9472
Vol. **1(6),** 40-45, December **(2012)** *Res. J. Engineering Sci.*

Review Paper

Modelling of ZnS:Mn AC Thin-Film Electroluminescent Devices

Tiwari Sanjay[1], Jain U.K.[2] and Tiwari Rameshwar[2]*
[1]S.O.S. in Electronics, Pt. Ravi Shankar Shukla, University, Raipur, CG, INDIA
[2]Department of Physics, Govt Postgraduate College, Chhindwara, MP, INDIA

Available online at: www.isca.in
Received 27th September 2012, revised 23rd October 2012, accepted 20th November 2012

Abstract

In this paper, previous and current approaches to alternating current thin-film electroluminescent (ACTFEL) device physics modeling are reviewed. Our aim of modeling of ACTFEL device is to accurately simulate the electrical properties of two-terminal ACTFEL test structures when subjected to realistic applied voltage waveforms. Additionally, modeling method that is believed to hold the most promise for accurate ACTFEL device modeling is presented. In this paper, a series of simple-to-complex models for device operation are offered that are useful for analysis in applications.

Keywords: Electroluminescence, tunneling effect, electron trapping, threshold voltage, modeling, modulation voltage.

Introduction

ACTFEL device is a thin-film stack typically consisting of a phosphor layer doped with a luminescent impurity which is sandwiched between two insulators that are in turn contacted by an opaque and a transparent electrode. An ACTFEL involves capacitive coupling between the electrodes and the phosphor. Capacitive coupling necessitates the use of the alternating current voltage waveform excitation which is applied between the two contacts to induce the light emission.

Basic Physical processes necessary for modeling of ACTFEL: The six basic processes responsible for ACTFEL operation which are summarized as follows: i. Injection : When sufficiently large voltage waveform is applied to the ACTFEL device, the phosphor field at the cathode/insulator interface is large enough that trapped interface state electrons are tunnel emitted into the phosphor conduction band. Where some of these electrons may inject from bulk traps and would lead to the formation of space charge in the phosphor and a concomitant non-uniform field across the phosphor[1]. Process (1) in figure 2 shows the re-emission of an electron back into the phosphor either through tunneling or from other process. This electron then drifts back across the phosphor due to the residual electric field until it is retrapped at the opposite interface or recombines with an ionized trap within the bulk phosphor. ii. Transport: Electrons injected into the phosphor conduction band gain energy from the electric field and are transported across the phosphor. It is possible that some of these electrons become sufficiently heated to induce electron multiplication in the phosphor via trap-to-band or band-to-band impact ionization[2,3] both trap-to-band and band-to-band impact ionization result in the creation of space charge in the phosphor again which would lead to curvature in the phosphor energy bands. iii. Impact ionization: As hot electrons transit the phosphor a fraction of them excite luminescent impurities from their ground state to the excited state from G to E[4] figure 1. iv. Radiative recombination: Relaxation of electron from the excited state back to its ground state results in photon emission[5]. Although this process can occur non-radiatively also[6]. v. Electron trapping: Transported electron reach the phosphor/insulator interface where they are trapped[7]. But in certain situations some of this trapping may also occur in bulk states near the anode/insulator interface. vi. Optical out-coupling: Photons generated via radiative recombination of luminescent impurities out-couple from the ACTFEL stack and are observed by the viewer[8].

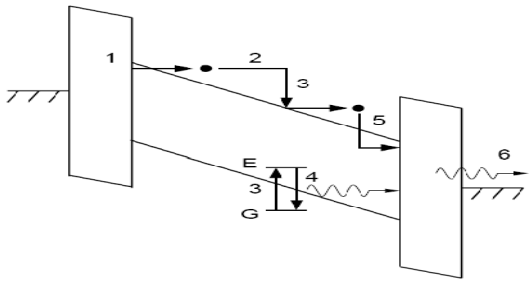

Figure-1
Basic processes which occur at applied voltages above threshold

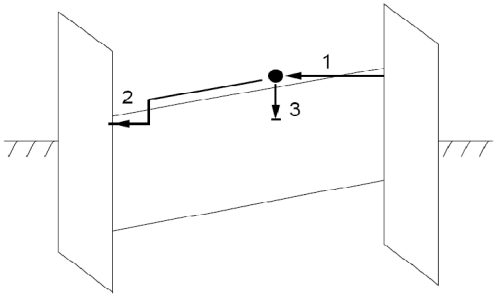

Figure-2
ACTFEL band structure during the Inter pulse interval

The credit of first effort to model ACTFEL devices goes to Chen and Krupka[9]. Their modeling approach involved writing device physics equations for the instantaneous field across and current through the phosphor layer in terms of the externally measured voltage and current. An effort was mode by Smith[10] to simulate the ACTFEL device. In this model, the insulators and phosphor layer are replaced by capacitances. The phosphor capacitance in then shunted by two back to back zener diode to account conduction across the phosphor. One of the important model was given by Davidson[11] and Massabrio[12]. Davidson used this model to compare the experimental and simulated C-V characteristic results for evaporated ZnS:Mn ACTFEL device. Douglas upgraded the Davidson's model after including a parallel RC network in series with the back-to-back zener diodes. This RC network accounts for the dependence of the turn-on voltage and relaxation charges on the applied voltage waveform and improves the simulated transient phosphor field trends. Aberg[13] developed a model to simulate the ALE, ZnS:Mn ACTFEL device. The model can be used to simulate ALE ZnS:Mn ACTFEL devices which do not exhibit L-V hysteresis. If the impedance is a resistor and capacitor in series, the model is capable to simulate the devices which exhibit L-V hysteresis. Finally, if the impedance is an inductor, the model can be used to account for dynamic space charge generation. De Carlo[14] presented state-space analysis to explain electrical characteristics of an ACTFEL device. First, the dynamic system is described by a small set of time dependent differential equations which provide information about the internal characteristics of the system. Second, the system is presumed to be describable by an nth order differential equation relating the internal state variables to the external, measurable output variables. Neyts[15] and Singh[16] have exclusively discussed the characterization and modeling of space charge in ACTFEL devices. Singh[17] developed an analytical model for yellow emitting ZnS:Mn, a.c. thin film electroluminescent (ACTFEL) display devices for yellow emitting ZnS:Mn Type AC Thin Film E1ectroluminescent Display Devices with Bulk Traps.

Proposed Model for Thin-Film EL Devices

The above arguments lead to the following simple equivalent-circuit model of the thin-film EL structure shown in Fig.3. Alt[18] demonstrated that this simple model contains the essential phenomenological physics of a thin-film EL device and in practice this model has been found to model accurately the most significant characteristics of a thin-film EL device. This model treats the insulating layers are incorporated into one effective insulating layer with the effective capacitance per unit area, $C_{I,}$ given by

$$C_I = \frac{C_{I1}C_{I2}}{C_{I1} + C_{I2}} \quad (1)$$

Where C_{I1} and C_{I2} are capacitances per unit area of the first and second insulating layers respectively. The thin film phosphor also behaves as a capacitor below the threshold voltage V_{th} with the capacitance per unit area C_{EL}. However, above the threshold voltage real (dissipative) current flows in the phosphor layer and gives rise to the light emission. Therefore, the phosphor layer is described as a capacitor in parallel with a non-linear resistor with the I-V characteristics shown in figure 4. In an ideal case, this non-linear resistor can be simulated by back-to-back Zener diodes. The luminance of the device is proportional to the power consumed in this resistive branch with the proportionality constant being the experimentally determined luminous efficiency η in units of lumens Per watt (lm/W).

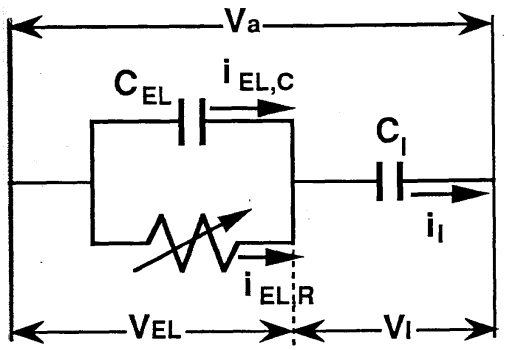

Figure-3

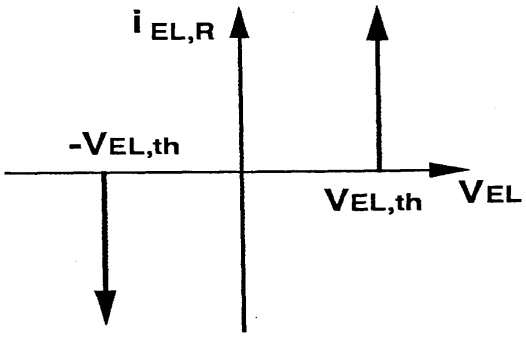

Figure-4

The analysis Alt[18] and King[19] that follows will first compute the transferred charge density in the resistive branch above the threshold voltage and the energy dissipated per unit area by this charge flow. The final solution will show the dependence of device performance on structure parameters such as layer thickness, dielectric constant, dielectric breakdown strength, threshold field, and luminous efficiency. Even though this model is certainly idealized, all the predicted dependencies are correct, and actual thin-film model is certainly designed with the help of this model.

First, let us define the symbols for the voltages across the device

$$V_a = V_I + V_{EL} \quad (2)$$

Where V_a is the voltage applied to the entire device, V_I is the portion of the voltage that appears across the insulating layers, and V_{EL} is the voltage across the phosphor (usually ZnS) layer. Below the threshold voltage these voltages are capacitively divided such that

$$V_{EL} = \frac{C_I}{C_I + C_{EL}} V_a \quad (3)$$

$$V_I = \frac{C_{EL}}{C_I + C_{EL}} V_a \quad (4)$$

Now suppose we apply the first pulse P_1 shown in figure 5 and that the magnitude of this pulse is greater than the threshold voltage V_{th}.

Initially the voltage across the layer is divided capacitively as given in Eqs. (3) and (4), so that

$$V_{EL,i1} = \frac{C_I}{C_I + C_{EL}} V_a \quad (3a)$$

$$V_{I,i1} = \frac{C_{EL}}{C_I + C_{EL}} V_a \quad (4a)$$

But now the resistive branch turns on the current flows (with accompanying light emission) to discharge the voltage across the phosphor capacitor back to the threshold level. At the same time the resistive branch must supply current to charge up the insulating layer capacitor by an equal voltage increment in order to maintain a constant voltage across the device. Thus we obtain

$$i_{EL,R} = i_I - i_{EL,C} \quad (5)$$

Where i_{EL}, R is the current of resistive part of the phosphor layer, i_{EL}, C is the current of capacitive part of the phosphor layer, and i_I is the current in the insulating layer. The final voltage values are

$$V_{EL,f} = V_{EL,th} = \frac{C_I}{C_I + C_{EL}} V_{th} \quad (6)$$

$$V_{I,f} = V_a - V_{EL,f} = \frac{C_{EL}}{C_I + C_{EL}} V_{th} \quad (7)$$

The voltage transferred ΔV_1 form the phosphor layer to the insulating layer is given by

$$\Delta V_1 = V_{EL,i} - V_{EL,f} = V_{I,f} - V_{I,i} = V_{EL,i} - V_{EL,th} \quad (8)$$

Or, in terms of the threshold voltage V_{th}

$$\Delta V_1 = \frac{C_1}{C_I + C_{EL}} (V_a - V_{th}) \quad (9)$$

The corresponding transferred charge per unit area, ΔQ_1, that flows in effecting the voltage transfer from the phosphor layer to the insulating layer is given by

$$\Delta Q_1 = C_I (\Delta V_1) \quad (10)$$

$$\Delta Q_{EL,C} = C_{EL} (-\Delta V_1) \quad (11)$$

$$\Delta Q_1 = \Delta Q_{EL,R} = \Delta Q_1 - \Delta Q_{EL,C} \quad (12)$$

Which leads to the final expression

$$\Delta Q_1 = C_1 (V_a - V_{th}) = \int_0^\infty i_{EL,R} dt \quad (13)$$

Equation 13 thus relates the internal real charge flow to the externally applied voltage and the insulating layer capacitance per unit area. This charge is transferred to the interface between the phosphor layer and the insulating layer and generates an internal electric field phosphor layer, E_{EL} to the threshold value, $E_{EL,th}$. When a second pulse of the same amplitude and polarity, pulse P_2, is applied, the initial voltage across the phosphor layer this time is

$$V_{EL,i2} = V_a - V_{I(previous)} = V_a - (V_a - V_{EL,th}) = V_{EL,th} \quad (14)$$

Thus, no conduction takes place and no light is emitted. The corresponding wave forms for these two pulses are shown in figure 5.

Now let up consider what happens when a pulse of the same amplitude and opposite polarity, pulse P_3 in figure 5, is applied and the stored charge at the interface has not decayed. Initially both the externally applied electric field and the field from the stored charge add to produce an internal field that is larger than the field associated with the first pulse. Thus more real charge must flow to discharge the voltage across the phosphor layer down to the threshold level. Therefore, the initial and final voltages across the phosphor layer are

$$V_{EL,i3} = \frac{\Delta Q_1}{C_I + C_{EL}} + \frac{C_I}{C_I + C_{EL}} V_a \quad (15)$$

$$V_{EL,f} = V_{EL,th} = \frac{C_I}{C_I + C_{EL}} V_{th} \quad (16)$$

and the transferred voltage for the pulse P_3, ΔV_3, is given by

$$\Delta V_3 = 2 \frac{C_I}{C_I + C_{EL}} (V_a - V_{th}) \quad (17)$$

or twice the value for the first pulse. The corresponding transferred charge density ΔV_3 is given by

$$\Delta Q_3 = 2 C_I (V_a - V_{th}) \quad (18)$$

Succeeding pulses of alternating polarity will also transfer this amount of voltage and charge density. In the steady state, the interface charge density at the end of a voltage pulse is one-half the transferred charge density: one-half the transferred charge neutralizes the previous interface charge, and the remaining half replaces it with an equal amount of opposite polarity. For a steady-state pulse-wave excitation, then, the transferred voltage ΔV and transferred charge density ΔQ are given by

$$\Delta V = 2\frac{C_I}{C_I + C_{EL}}(V_a - V_{th}) \quad (19)$$

$$\Delta Q = 2C_I (V_a - V_{th}) \quad (20)$$

Next let us calculate the work done per unit area and power consumption (input power) per unit area in this model. To first approximation all real charge is transported across the phosphor layer of thickness d_{EL} at the threshold field, $d_{EL,th.}$ Thus the work done per unit area, W, is given by

$$W = 2C_I (V_a - V_{th}) E_{EL,th} d_{EL} = 2C_I (V_a - V_{th}) V_{EL,th} \quad (21)$$

Since this transport occurs twice a cycle, the power consumption per unit area, or input power density into an EL device, $P_{in,}$ is given by

$$P_{in} = 4fC_I (V_a - V_{th}) V_{EL,th} \quad (22)$$

The luminance is then computed by multiplying Eq. 22 by the experimentally determined luminous efficiency, η as

$$L = \frac{1}{\pi}\eta P_{in} = \frac{4}{\pi} nfC_I (V_a - V_{th}) V_{EL,th} \quad (23)$$

Here π in the denominator comes from the assumption of perfectly diffusive surface of EL device. The above equation for luminance assumes a number of simplifications. The luminous efficiency is assumed to be independent of the electric field and phosphor thickness. Experimentally, luminous efficiency does increase with thickness at least over a limited range of thickness. It also assumes that all charge is transferred at $d_{EL,\,th}$, when, in fact, charge will flow at higher voltages, depending on the voltage rise time.

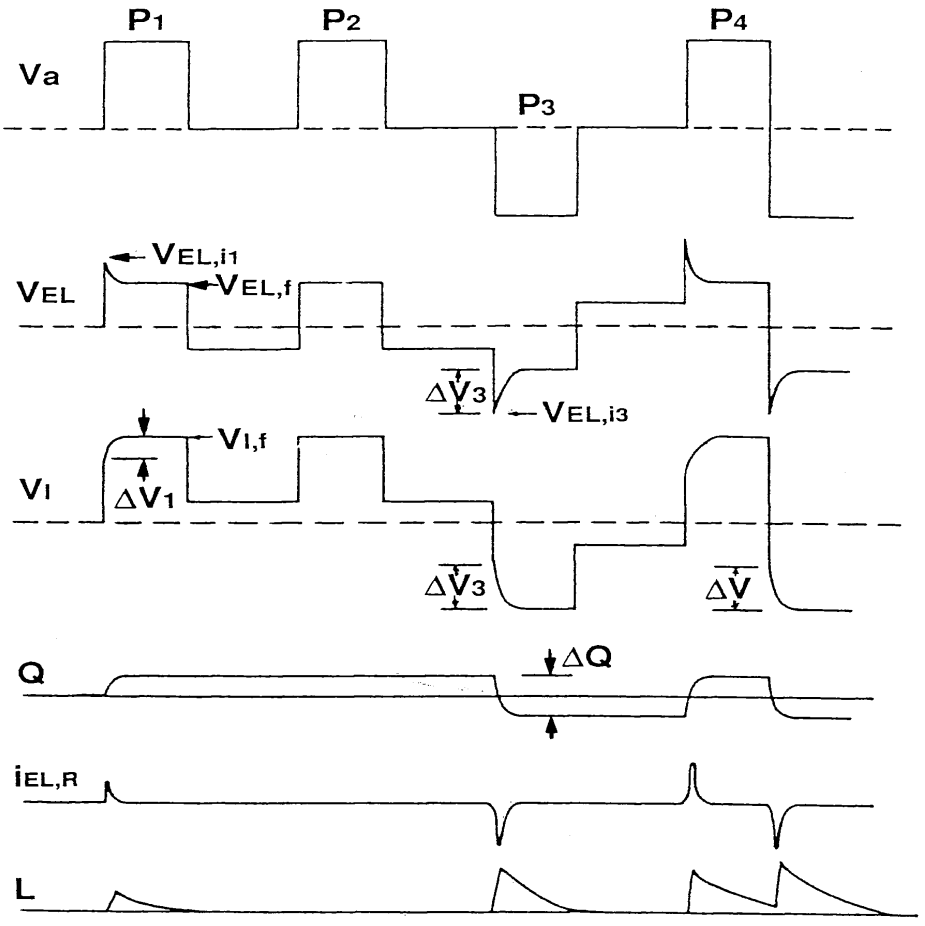

Figure-5

Now we rewrite equation 23 in a form that directly shows how the structure parameters influence device performance. Using the relationships

$$C_I = \frac{\varepsilon_0 \varepsilon_I}{d_I} \quad (24)$$

$$V_{EL,th} = E_{EL,th}\, d_{EL,th} \quad (25)$$

Where ε_0 is the dielectric constant of the vacuum and ε_I is the relative dielectric constant of insulating layer material. Then equation 23 becomes

$$L = \frac{4}{\pi}\eta f \varepsilon_0 \varepsilon_I \left(\frac{d_{EL}}{d_I}\right) E_{EL,th}\left(V_a - V_{th}\right) \quad (26)$$

Thus in order to optimize the luminance of the EL device with a constant modulation voltage $(V_a - V_{th})$, the relative thickness of the phosphor layer to the insulating layer should be maximized and the insulating layer should have a high dielectric constant. The remainder of the terms in the equation is essentially constant. If one is willing to increase the modulation voltage, V_a – V_{th}, the luminance can be increased further. However, this has two practical limitations. First the major component of the power consumption increases as the square of modulation voltage. Second the dielectric breakdown of the insulating layer places a reliability limit on this voltage. To see this we rewrite equation 13 using equation 12.

$$V_a - V_{th} = \frac{\Delta Q_I - \Delta Q_{EL,C}}{C_I} \quad (27)$$

Which states that all the voltage above threshold are transferred to the insulating layer. Thus the maximum voltage excursion is limited by the dielectric breakdown electric field of the insulating layer, E_{BD}, or alternately its maximum charge density capacity, ΔQ_{max} which is equal to $\varepsilon_0 \varepsilon_I E_{BD}$. This term was first introduced by Howard. $\Delta Q_{EL,C}$ is the charge on the phosphor layer at the threshold. Thus equation 21 becomes

$$L = \frac{4}{\pi}\eta f d_{EL} E_{EL,th}\left(\Delta Q_I - \Delta Q_{EL,C}\right) \quad (28)$$

In this form it is obvious that the luminance increases with the phosphor layer thickness a level which is only limited by the insulating layer charge density capacity.

Conclusion

Previous and current approaches to alternating current thin-film electroluminescent (ACTFEL) device physics modeling are reviewed in this paper, our aim of modeling of ACTFEL device to accurately simulate the electrical properties of two-terminal ACTFEL test structures when subjected to realistic applied voltage waveforms is successfully achieved by proposing model. The proposed model shown in figures 3 and 4 accounts for most of the observed thin-film EL device characteristics and can be used in quantitative calculations to predict device performance. However, there is one aspect of device performance not accurately presented by this simple proposed model and that is the time dependence of the charge transport. A comprehensive review of previous ACTFEL modeling efforts is presented. Additionally, modeling method that is believed to hold the most promise for accurate ACTFEL device modeling has been developed. Special consideration is given to the role of tunneling and space charge in determining the electrical characteristics and to the special features of the Mn^{++} center in ZnS. It is suggested that an Auger process involving this center can provide a link between concentration quenching and the occurrence of hysteresis or memory effect. The nature of brightness saturation in ZnS:Mn devices is reviewed. The saturation data strongly suggest an interaction between Mn^{++} excited states that provide nonradiative decay channels.

References

1. Hitt J.C., Bender J.P. and Wager J.F., Thin-Film Electroluminescent device Physics Modeling, Critical Rev. in Solid State and Material Science, **25(1)**, 29-85 **(2000)**

2. Bhattacharyya K., Goodnich S.M. and Wager J.F., Monte Carlo simulation of electron transport in alternating-current Thin-Film Electroluminescent devices, *J. Applied Physics*, **73(7),** 3390-3396 **(1993)**

3. Raker T., Kuhn T., Kuligk A., Fitzer N., Redmer R., Zuccaro S., Niederno F.J. and Purwins H.G., High-field Transport in Ac Thin-film EL Devices, Theory and experiment Physics B Condensed Matter, **314(1-4)**, 185 **(2002)**

4. Bringuier E. and Geoffroy A., Charge transfer in ZnS-type electroluminescence revisited, *Appl. Phys. Lett*., **60(10)**, 1256-1258 **(1992)**

5. Blasse G. and Grabmaier B.C., Luminescent Materials, Springer-Verlag, Berlin **(1994)**

6. Mach R. and Muller G.O., Ballistic transport and electroluminescence in IIB-VI and IIA-VI, *J. Crystal Growth*, **100(1)**, 967-975 **(1990)**

7. Wolf S. and Tauber R.N., Silicon Processing for the VLSI Era, Lattice Press, California**, 1 (1986)**

8. Ylilammi M., Optical Properties of ACTFEL Displays, **3(2)**, 56-66 **(1995)**

9. Chen Y.S. and Krupka D.C., Limitation imposed by field clamping on the efficiency of high-field ac electroluminescence in thin films, *J. Appl. Phys*., **43(10)**, 4089-4096 **(1972)**

10. Smith D.H., Modeling of ac thin-film Electroluminescent Devices, *J. of Luminescence*, **23(1-2)**, 209-235 **(1981)**

11. Davidson J.D., Wager J.F., Khormaei R.I., King C.N. and Williams R., Electrical characterization and modeling of alternating-current thin-film electroluminescent devices, IEEE Trans. Electron Devices, **39(5)**, 1122-1128 **(1992)**

12. Massabrio G. and Antognetti P., Semiconductor Device Modeling with SPICE, New York: McGraw-Hill, Inc **(1993)**

13. Aberg M., An Electroluminescent Display Simulation system and its application for developing grey scale dividing methods, Ph. D. Thesis, Helsinki University, *Technol. Espoo. Finland*, **(1993)**

14. Decarlo R.C., Limitation imposed by field clamping on the efficiency of high-field ac electroluminescence in thin films, *J. Appl. Phys.,* **43(10)**, 4089-4096 **(1972)**

15. Neyts K.A. and Coriatan D., Simulation and measurement of multiplication in thin-film electroluminescent devices with doped probe layers, IEEE Trans. Electron Devices, **45(4)**, 768-777 **(1998)**

16. Singh V.P., Krishna S. and Morton D.C., Electric field and conduction current in ac thin-film electroluminescent display devices, *J. Appl. Phys*., **70(3)**, 1811-1920 **(1991)**

17. Singh V.P., Majid W. and Morton D., Analysis of ZnS:Mn type ac thin-film electroluminescent display devices with bulk traps, *J. Soc. Inf. Display*, **1(2)**, 135-141 **(1993)**

18. Alt P.M., Thin-film electroluminescent displays: device characteristics and performance, Proc. SID, **25(2)**, 123-146 **(1984)**

19. King C.N., Thin-film electroluminescent displays, Society for Information Display Seminar Lecture Notes, **1S,** 4.1/1 - 4.4/1 **(1985)**